Earth and Planetary Science Letters 310 (2011) 441–452

Contents lists available at SciVerse ScienceDirect

Earth and Planetary Science Letters

journal homepage: www.elsevier.com/locate/epsl

Magnetotactic bacterial abundance in pelagic marine environments is limited by organic carbon flux and availability of dissolved iron

Andrew P. Roberts [a,b,*], Fabio Florindo [c], Giuliana Villa [d], Liao Chang [a], Luigi Jovane [a,c], Steven M. Bohaty [a], Juan C. Larrasoaña [e], David Heslop [b], John D. Fitz Gerald [b]

[a] National Oceanography Centre, University of Southampton, Southampton SO14 3ZH, UK
[b] Research School of Earth Sciences, The Australian National University, Canberra, ACT 0200, Australia
[c] Istituto Nazionale di Geofisica e Vulcanologia, Via di Vigna Murata 605, 00143 Rome, Italy
[d] Dipartimento Scienze della Terra, Università di Parma, Viale Usberti 157A, 43100 Parma, Italy
[e] Área de Cambio Global, IGME, Oficina de Proyectos de Zaragoza, Manuel Lasala 44 9B, Zaragoza 50006, Spain

ARTICLE INFO

Article history:
Received 26 April 2011
Received in revised form 2 August 2011
Accepted 9 August 2011
Available online xxxx

Edited by P. DeMenocal

Keywords:
Magnetotactic bacteria
Magnetofossils
Magnetite
Productivity
Iron
Organic carbon

ABSTRACT

Magnetotactic bacteria intracellularly biomineralize magnetite of an ideal grain size for recording palaeomagnetic signals. However, bacterial magnetite has only been reported in a few pre-Quaternary records because progressive burial into anoxic diagenetic environments causes its dissolution. Deep-sea carbonate sequences provide optimal environments for preserving bacterial magnetite due to low rates of organic carbon burial and expanded pore-water redox zonations. Such sequences often do not become anoxic for tens to hundreds of metres below the seafloor. Nevertheless, the biogeochemical factors that control magnetotactic bacterial populations in such settings are not well known. We document the preservation of bacterial magnetite, which dominates the palaeomagnetic signal throughout Eocene pelagic carbonates from the southern Kerguelen Plateau, Southern Ocean. We provide evidence that iron fertilization, associated with increased aeolian dust flux, resulted in surface water eutrophication in the late Eocene that controlled bacterial magnetite abundance via export of organic carbon to the seafloor. Increased flux of aeolian iron-bearing phases also delivered iron to the seafloor, some of which became bioavailable through iron reduction. Our results suggest that magnetotactic bacterial populations in pelagic settings depend crucially on particulate iron and organic carbon delivery to the seafloor.

1. Introduction

Magnetotactic bacteria represent a heterogeneous group of prokaryotes that mineralize membrane-enclosed iron minerals known as magnetosomes (e.g., Bazylinski and Frankel, 2004; Faivre and Schüler, 2008; Kopp and Kirschvink, 2008). These biomineralized particles have ideal magnetic single domain (SD) sizes that produce strong magnetizations. Magnetosomes align in chains, with chain orientation close to the axis of cell motility. By rotating helical flagella, the bacteria use the magnetosomes to orient themselves and navigate using the local geomagnetic field. The ability to align parallel to geomagnetic field lines is known as magnetotaxis, from which the term 'magnetotactic' arises. Most magnetotactic bacteria are found in chemically stratified water columns or sediments; they are gradient organisms that derive energy for growth from the proximity of reductants and oxidants around thin layers at specific locations near chemical interfaces (Bazylinski and Frankel, 2004; Faivre and Schüler, 2008; Flies et al., 2005; Kopp and Kirschvink, 2008). In microaerobic environments, magnetosomes consist of magnetite (Fe_3O_4), whereas greigite (Fe_3S_4) is found in magnetotactic bacteria from sulphidic environments (Bazylinski et al., 1993).

Prevalence of microaerobic or anoxic conditions is crucial for magnetotactic bacterial biomineralization (Blakemore et al., 1985; Schüler and Baeuerlein, 1998). Higher oxygen concentrations suppress magnetite biomineralization or result in formation of smaller and aberrantly shaped crystals (Bazylinski and Frankel, 2004; Faivre and Schüler, 2008). Magnetotactic bacteria are abundant in coastal marine settings, but they also occur at water depths down to and exceeding 4500 m (Hesse, 1994; Housen and Moskowitz, 2006; Petermann and Bleil, 1993; Stoltz et al., 1986). The widespread distribution of magnetotactic bacteria in marine environments means that when they die, magnetosomes can be buried and fossilized. As SD particles, magnetosomes are ideal palaeomagnetic recorders; they have therefore been argued to be widely responsible for palaeomagnetic signals in the sedimentary record (e.g., Kirschvink, 1982; Petersen et al., 1986; Stoltz et al., 1986; Vali et al., 1987). However, their small particle size means that magnetosomes tend to dissolve when buried under anoxic conditions (e.g., Faivre and Schüler, 2008; Housen and Moskowitz,

* Corresponding author at: Research School of Earth Sciences, The Australian National University, Canberra, ACT 0200, Australia.
E-mail address: andrew.roberts@anu.edu.au (A.P. Roberts).

0012-821X/$ – see front matter © 2011 Elsevier B.V. All rights reserved.
doi:10.1016/j.epsl.2011.08.011

2006; Kopp and Kirschvink, 2008; Tarduno, 1994). Magnetofossils have therefore only been reported as the dominant carrier of palaeomagnetic signals in a few pre-Quaternary locations (Kopp and Kirschvink, 2008).

In marine environments, magnetofossils are most commonly reported in carbonates that lack significant terrigenous particle concentrations (e.g., Petersen et al., 1986; Vali et al., 1987). Calcareous oozes are deposited on almost 50% of the global seafloor, so there is considerable potential for magnetosome production and subsequent preservation of magnetofossils in carbonate sediments. However, iron is a limiting micronutrient for phytoplankton productivity in surface waters within oligotrophic oceanic gyres (Boyd and Ellwood, 2010; Jickells et al., 2005; Martin et al., 1991). Even though dissolved iron is usually more abundant in bottom waters compared to surface waters (e.g., Boyd and Ellwood, 2010), bioavailable iron required for biomineralization by magnetotactic bacteria is still typically only present in extremely low (nanomolar and lower) concentrations. Organic-rich near-coastal environments are more likely to support the diagenetic iron redox cycling needed to provide iron for uptake by magnetosomes (Bazylinski et al., 2007), but they are also likely to have reducing diagenetic conditions at shallow depths in the sediment column with poor preservation potential for magnetofossils. Assessing the production and preservation of magnetotactic bacteria and their role in the magnetization of sediments requires knowledge of the interplay between nutrient limitations, organic carbon flux and palaeoproductivity, climate, iron bioavailability, redox environment, and sediment magnetism. This interplay is poorly understood in deep-sea environments where relatively few studies have been made (e.g., Dinarès-Turell et al., 2003; Hesse, 1994; Lean and McCave, 1998; Tarduno, 1994; Tarduno and Wilkison, 1996; Yamazaki and Kawahata, 1998) compared to coastal settings. The presence or absence of magnetofossils is also important for preserving a palaeomagnetic signal in otherwise weakly magnetized pelagic carbonates, which is crucially important for constructing geomagnetic polarity chronologies and for investigating environmental changes in the geological record.

Electron paramagnetic resonance (EPR) spectra (Weiss et al., 2004; Kopp et al., 2006), first-order reversal curve (FORC) diagrams (Egli et al., 2010; Pike et al., 1999; Roberts et al., 2000), and transmission electron microscope (TEM) observations enable detection of magnetosome chains within sediments, even when other magnetic minerals are present. We use these techniques to delineate the temporal distribution of magnetofossils in Eocene sediments from Ocean Drilling Program (ODP) Hole 738B (Fig. 1) and to better understand the factors that control magnetotactic bacterial activity in deep-sea environments.

2. Methods

We analysed samples from ODP Hole 738B (62°42, 54′S; 82°47, 25′E; 2253 m water depth; 1750 m palaeo water depth; Fig. 1). ODP Hole 738B was sampled for magnetic analysis with 8-cm^3 plastic cubes (146 samples) that were collected from the working half of cores 738B-3H to 12H (16.52–103.46 m below seafloor (mbsf)) at an average spacing of 60 cm. An isothermal remanent magnetization (IRM) was imparted with a pulse magnetizer in stepwise increasing fields up to 900 mT and was measured at the Istituto Nazionale di Geofisica e Vulcanologia (INGV), Rome, Italy, using a 2-G Enterprises cryogenic magnetometer with in-line AF demagnetizer. The high coercivity magnetization component due to hematite was estimated by subtracting the IRM imparted at 900 mT from that imparted at 300 mT ($IRM_{900\ mT} - IRM_{300\ mT}$). IRM acquisition, backfield demagnetization, hysteresis and FORC measurements were made on further selected samples using a Princeton Measurements Corporation vibrating sample magnetometer at the National Oceanography Centre (NOC), Southampton, UK, with peak applied fields up to 1 T. IRM acquisition curves were separated into different coercivity

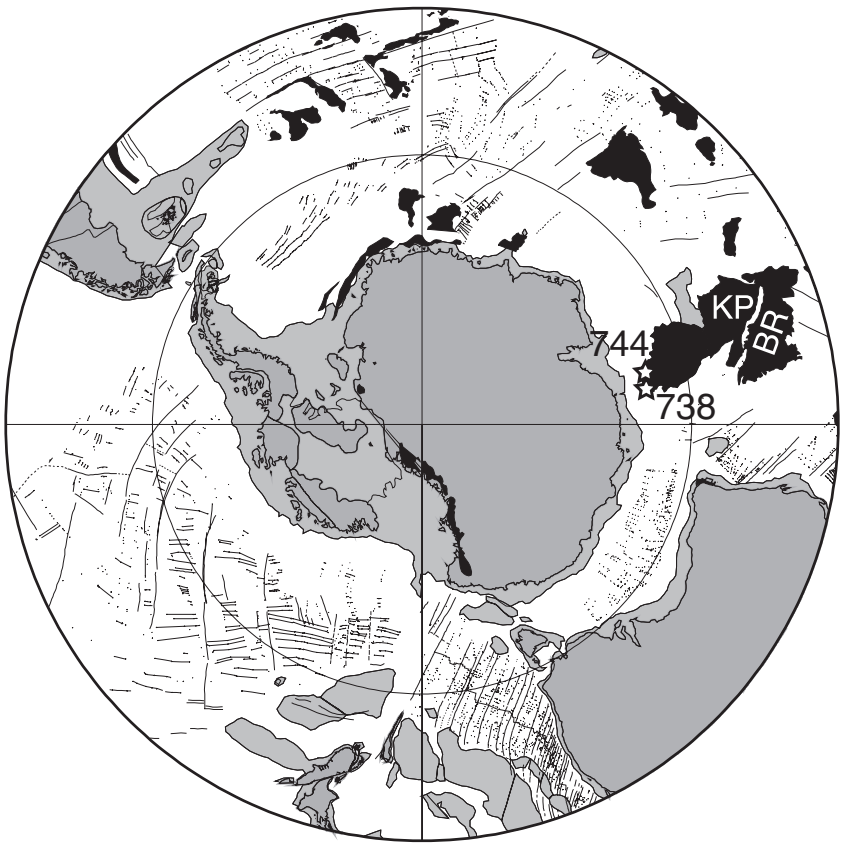

Fig. 1. Plate reconstruction of the Southern Ocean during the Middle Eocene (after Lawver and Gahagan, 2003) with location of the studied ODP sites (738 and 744) from the southern Kerguelen Plateau, Indian Ocean (polar stereographic projection to 45°S). Black areas are large igneous provinces (after Eldholm and Coffin, 2000), light shaded areas are continental shelves, darker lines are magnetic isochrons and fracture zone lineations, and lighter lines are plate boundaries (KP = Kerguelen Plateau, BR = Broken Ridge).

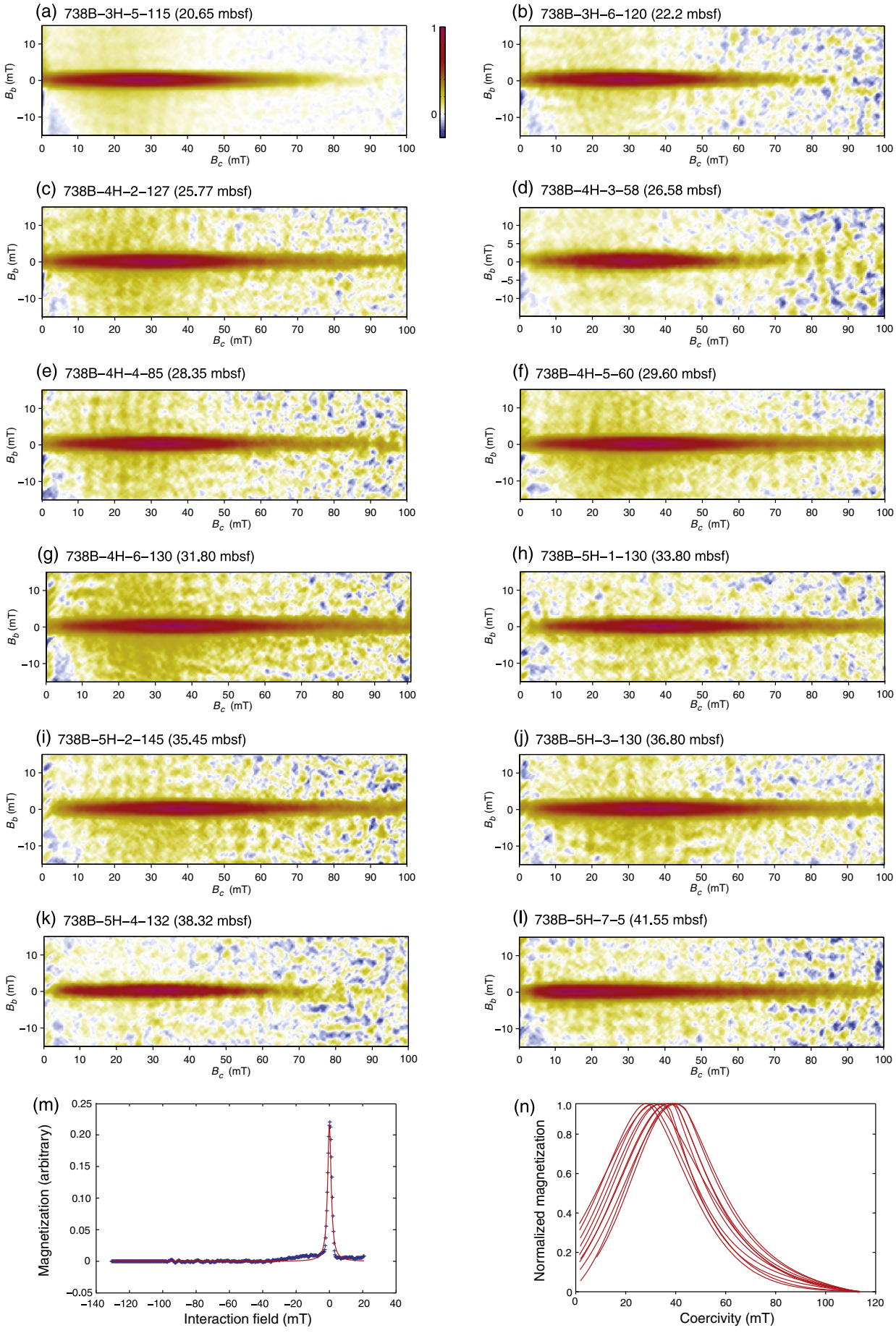

spectra (e.g., Robertson and France, 1994) using the IRM unmixing procedure of Heslop et al. (2002). Before unmixing analysis was performed, individual stepwise IRM acquisition curves were smoothed using a constrained least-squares spline (de Boor, 1994). The derivative of the spline function was then modelled using three log-Gaussian distributions that are assumed to represent separate coercivity components (Robertson and France, 1994). The optimal distribution parameters (M_r, $B_{1/2}$ and DP) for each sample were determined using the algorithm of Heslop et al. (2002). For FORC measurements, up to 247 FORCs were measured with averaging times of 250 to 500 ms depending on the strength of the sample magnetization. FORC diagrams were produced with a smoothing factor (SF) of 5 (Roberts et al., 2000) using the software of Egli et al. (2010). FORCs were measured with small field steps to enable detection of features associated with intact magnetofossil chains (Egli et al., 2010).

EPR spectroscopy is used to probe unpaired electrons within samples and has recently been developed to detect the magnetic anisotropy associated with magnetosome chain structures within bulk sediment samples (Kopp et al., 2006; Weiss et al., 2004). We measured EPR spectra on bulk carbonates from ODP Hole 738B to detect magnetofossils using an X-band Bruker EMX microspectrometer at the School of Chemistry, University of Manchester, UK. For each measurement, ~100–200 mg of air-dried sediment was loaded into EPR glass tubes. We used a microwave frequency of ~9.4 GHz and microwave power of ~0.632 mW. All spectra were integrated over three magnetic field sweeps from 0 to 700 mT.

For selected samples, the magnetic mineralogy was studied at the INGV by measuring the low-field magnetic susceptibility during heating to 700 °C using a Kappabridge KLY-3 magnetic susceptibility meter with CS-3 heating attachment. Magnetic mineral extracts were obtained following adaptations of the methods of Stoltz et al. (1986) and Hesse (1994) and were imaged and analysed using a Philips CM300T TEM operated at 300 kV in the Research School of Earth Sciences at the Australian National University. This instrument is equipped with an EDAX Phoenix retractable X-ray detector (ultra-thin window) and a Gatan model 694 slow-scan digital camera.

Finally, we use calcareous nannofossils, which dominate the studied sediments, as palaeoenvironmental indicators. Nannofossil census data were collected from Site 738 as part of a biostratigraphic study for the late Middle Eocene to the earliest Oligocene (Persico et al., 2011) following previous studies of Southern Ocean sites (e.g., Persico and Villa, 2004; Villa et al., 2008) in which abundance variations were counted for oligotrophic, eutrophic, temperate, warm, and cool water taxa. This approach provides useful information concerning surface water nutrient conditions at the time of sediment deposition. Faul and Delaney (2010) also reported nutrient proxy data for Site 738, but their low-resolution study only has a few samples in the interval of interest for this study, so we rely on nutrient information provided by calcareous nannofossil census data.

3. Results

Throughout the Eocene, the southern Kerguelen Plateau and ODP Site 738 (Fig. 1) was dominated by pelagic biogenic sedimentation (mainly calcareous nannofossil and foraminiferal oozes). Several observations provide evidence that magnetite magnetofossils are preserved throughout the studied sedimentary sequence at Hole 738B. FORC distributions are nearly identical for all samples studied (Fig. 2a–l), with a sharply peaked vertical distribution (Fig. 2m) and coercivity distribution peaks between 17 and 30 mT (Fig. 2n). The sharp vertical peak of the FORC distributions (Fig. 2m) indicates a dominance of non-interacting particles (Roberts et al., 2000) and is characteristic of intact magnetosome chains (Egli et al., 2010). The weaker outer parts of the FORC distributions indicate minor but variable contributions from coarser-grained particles (Roberts et al., 2000). The coercivity distributions (Fig. 2n) fall within the range expected for magnetite magnetosomes (Egli, 2004a; Kopp and Kirschvink, 2008).

All measured EPR spectra contain sharp lines (6 intense and 10 weak lines; Fig. 3a, c), which are due to Mn^{2+} in calcite (e.g., Boughriet et al., 1992; Otamendi et al., 2006). In order to remove the strong Mn^{2+} sextet signals and to analyse the broad EPR signal, we used a Fast Fourier Transform to filter the high-frequency signals from the measured EPR spectra. The broad EPR spectra are associated with magnetically ordered minerals: they have two clear maxima at low applied fields and are asymmetrically extended to the low field direction (Fig. 3a). The shapes of the measured EPR spectra are distinctive of intact magnetite magnetosome chains (Charilaou et al., 2011; Fischer et al., 2008; Kopp et al., 2006; Weiss et al., 2004). We use the EPR parameters defined on Fig. 3b (Kopp et al., 2006) to describe the spectra. Values of g_{eff} are consistently 1.95–1.99 (Table 1), which fall within the range $g_{eff}<2.12$ for almost all published samples that contain magnetite magnetosomes. A is much lower than 1 (Table 1), which suggests that the spectra shift to lower fields. Kopp et al. (2006) proposed that values of their α parameter <0.3 indicate the presence of biogenic magnetite chains. For our samples, $\alpha = 0.24$–0.29 (Table 1). The shape of EPR spectra, and parameters derived from the spectra (Kopp et al., 2006; Weiss et al., 2004), and high-resolution FORC diagrams (Egli et al., 2010) are all therefore indicative of intact magnetite magnetosome chains throughout the studied interval of Hole 738B.

Transmission electron microscope (TEM) observations of magnetic extracts confirm the presence of magnetite magnetofossils (Fig. 4), with a variety of morphologies including octahedra, cubo-octahedra, and hexagonal prisms that are typical of magnetosome crystals reported from living magnetotactic bacteria (Kopp and Kirschvink, 2008). The collective evidence provides maximum scores in the full range of tests proposed by Kopp and Kirschvink (2008) for magnetosome identification.

Temperature-dependent susceptibility data provide evidence for the presence of significant concentrations of hematite (Néel temperature of 680 °C) in addition to magnetite (Fig. 5), which, as demonstrated above, has a bacterial origin. Magnetic hysteresis data (Fig. 6a) plot close to the data field for ideal SD magnetic particles (Day et al., 1977), as expected for mixtures of fossil magnetosomes and coarser-grained detrital magnetic particles. The presence of mixtures of high-coercivity hematite with lower coercivity bacterial magnetite is supported by stepwise IRM acquisition and backfield demagnetization curves (Fig. 6b, c). Curves that saturate rapidly are dominated by bacterial magnetite, while those that saturate more slowly contain progressively greater admixtures of hematite.

Three magnetic components are identified in all studied samples (Fig. 7). The lowest coercivity component (component 1 in Table 2) has a broad coercivity distribution (Fig. 7), as indicated by high values of the dispersion parameter (DP) of Robertson and France (1994). This component is interpreted to represent relatively coarse-grained magnetite, which is consistent with the interpretations of Egli (2004b). The high coercivity hematite component (cf. Fig. 5) has variable coercivity. We therefore separate it into two variable components (Fig. 7; components 3 and 4 in Table 2), but each sample has only one hematite component and no sample has more than three components in total. The soft magnetite and the hematite components are probably aeolian in

Fig. 2. FORC diagrams for samples from ODP Hole 738B. (a–l) The FORC diagrams are consistently dominated by a sharp ridge centred on $B_b = 0$, which is indicative of non-interacting SD magnetic particles (Roberts et al., 2000). (m) Vertical profile through the peak of the FORC distribution, fitted with a Lorentzian function. The sharpness of the ridge indicates a lack of magnetostatic interactions, which is consistent with the presence of intact magnetosome chains (Egli et al., 2010). (n) Coercivity (B_c) distributions through the peak of the FORC distributions for 10 samples through the studied interval of Hole 738B. The distribution peaks occur between 17 and 30 mT, which is within the range of values for bacterial magnetite (Egli, 2004a; Kopp and Kirschvink, 2008). The scale beside (a) provides a normalized measure of magnetization. The smoothing factor (Roberts et al., 2000) is 5 in all cases.

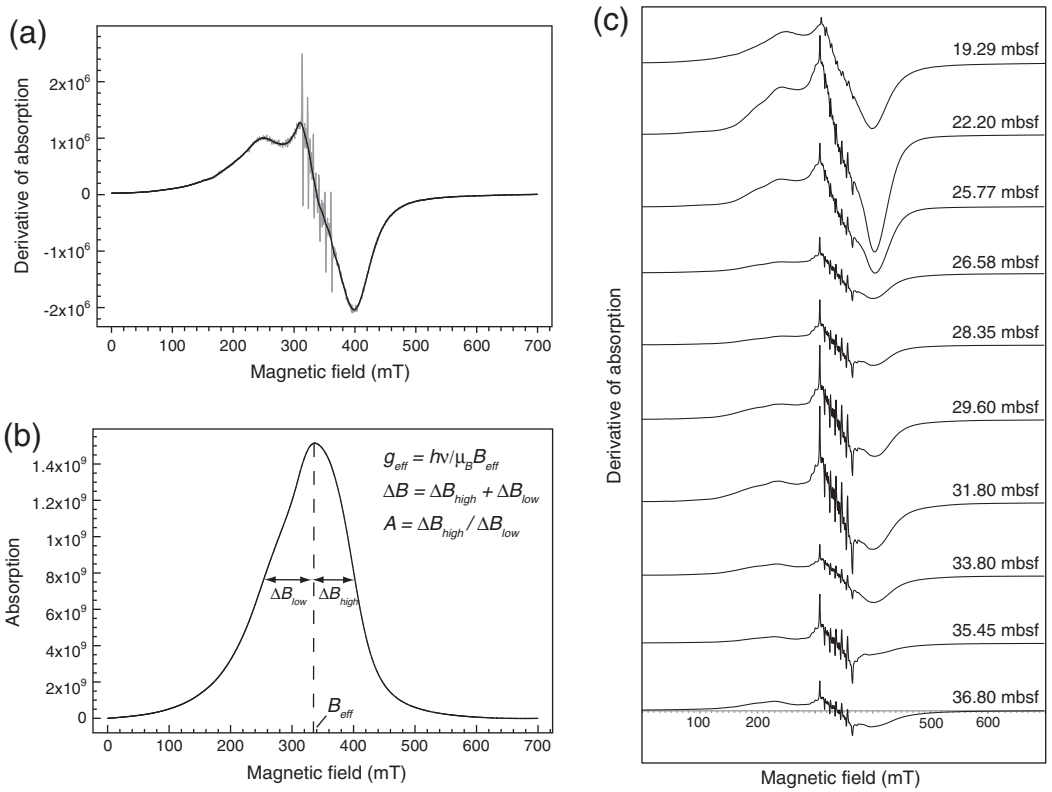

Fig. 3. EPR spectra for measured samples from ODP Hole 738B, which provide strong evidence for the presence of intact fossil magnetosome chains. (a) Representative EPR spectrum for a sample from Hole 738B. The grey line represents the measured data, while the black curve fit represents the spectrum after filtering of the high frequency signal using a Fast Fourier Transform. This treatment has not evidently distorted the key features of the EPR signal. (b) Idealized (smoothed) EPR absorption spectrum with definition of parameters (see Table 1) used to assess the presence of magnetite magnetofossils. As discussed in the text, these values are consistent with those of intact magnetosome chains. (c) Down-hole progression of EPR spectra for samples between depths of 19.29 and 36.80 mbsf. Each spectrum has been normalized by sample mass so that the respective spectra can be compared directly as shown.

origin. The dominant magnetic component in each sample is due to magnetite magnetofossils, as demonstrated above (Fig. 7; component 2 in Table 2). It has relatively consistent coercivity and low dispersion (Table 2). This component has properties that match those of the "biogenic soft" component of Egli (2004b). We observe no component with the properties expected for the "biogenic hard" component of Egli (2004b).

Magnetite saturates in an applied field of 300 mT; any magnetization acquired above 300 mT therefore provides a measure of the high coercivity mineral content, which in this case is carried by hematite (cf. Fig. 5). The contribution of hematite (Fig. 8a) is therefore estimated using $IRM_{900\ mT} - IRM_{300\ mT}$. For the samples listed in Table 2, 55–80% of the IRM is carried by magnetite magnetofossils. We therefore treat the large-scale IRM variations as dominantly indicating major fluctuations in bacterial magnetite concentrations at Site 738 (Fig. 8b). As is evident from the values of $IRM_{900\ mT} - IRM_{300\ mT}$ and $IRM_{900\ mT}$ (Fig. 8a, b), the former parameter is at least 2 orders of magnitude weaker than $IRM_{900\ mT}$. However, the spontaneous magnetization of hematite is

Table 1
Measured hysteresis and electron paramagnetic resonance parameters for the studied sediments from ODP Hole 738B.

Sample	Depth (mbsf)	M_r (Am^2)	M_s (Am^2)	M_r/M_s	B_c (mT)	B_{cr} (mT)	B_{cr}/B_c	g_{eff}	B_{low} (mT)	B_{high} (mT)	ΔB_{low} (mT)	ΔB_{high} (mT)	B_{eff} (mT)	ΔB_{FWHM} (mT)	A	α
738B-3H-4-129	19.29							1.99	253.1	402.5	84.1	65.3	337.2	149.4	0.77630	0.28
738B-3H-5-115	20.65	1.358	3.243	0.419	20.19	30.65	1.518	1.99	261.9	403.9	75.2	66.7	337.2	141.9	0.88623	0.29
738B-3H-6-120	22.2	1.169	2.753	0.425	20.93	31.71	1.515	1.99	261.9	403.9	75.9	66.0	337.9	141.9	0.86934	0.29
738B-4H-2-127	25.77	0.915	2.024	0.452	27.84	45.17	1.622	1.98	252.4	404.2	86.9	65.0	339.2	151.8	0.74799	0.28
738B-4H-3-58	26.58	0.651	1.492	0.436	26.14	40.92	1.565	1.99	262.6	400.1	74.9	62.6	337.5	137.5	0.83563	0.28
738B-4H-4-85	28.35	0.786	1.802	0.437	27.69	41.96	1.515	1.98	256.8	401.8	82.8	62.2	340.0	145.0	0.75193	0.27
738B-4H-5-60	29.6	0.917	2.006	0.457	28.48	44.08	1.548	1.97	252.0	402.8	88.6	62.2	340.6	151.0	0.70227	0.27
738B-4H-6-130	31.8	1.247	2.739	0.455	30.18	45.94	1.522	1.95	241.4	408.0	102.9	63.6	344.4	166.5	0.61790	0.27
738B-5H-1-130	33.8	0.501	1.049	0.478	33.59	49.6	1.477	1.97	258.9	393.6	81.4	53.3	340.3	134.7	0.65557	0.24
738B-5H-2-145	35.45	0.803	1.707	0.470	33.75	50.41	1.494	1.96	235.3	407.3	106.7	65.3	342.0	172.0	0.61224	0.27
738B-5H-3-130[a]	36.8	0.589	1.234	0.477	29.18	42.08	1.442									
738B-5H-4-132	38.32	0.289	0.623	0.463	24.07	35.43	1.472	1.99	271.5	390.2	66.7	52.0	338.2	119.0	0.77954	0.25
738B-5H-5-131[a]	39.81	0.018	0.042	0.426	27.42	39.61	1.445									
738B-5H-7-5	41.55	0.609	1.255	0.485	22.48	36.36	1.617	1.96	271.5	393.9	70.4	52.0	342.0	122.4	0.73793	0.25

[a] No EPR data reported due to noisy spectra.

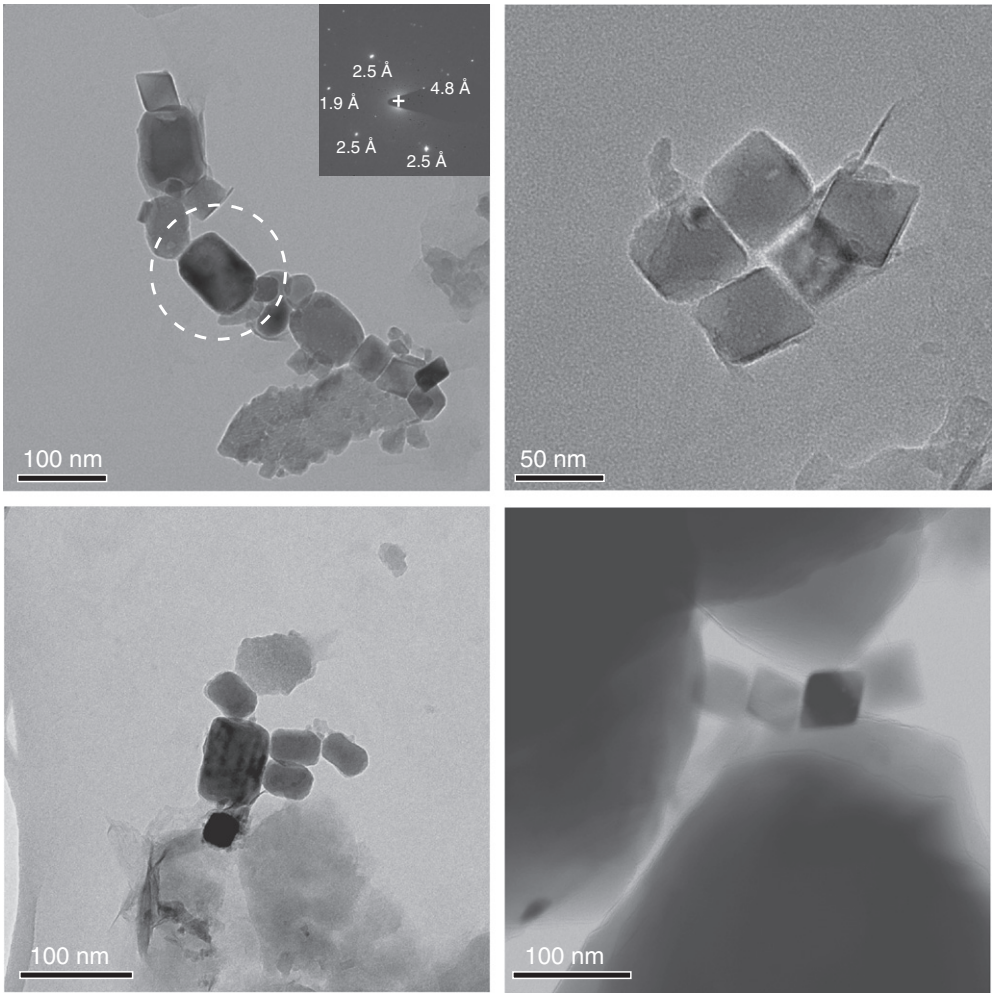

Fig. 4. TEM images for a magnetic mineral extract containing direct evidence of fossil magnetosomes (sample 738B-5H-2-101 cm; 35.01 mbsf). The biogenic magnetite particles have a range of typical magnetosome morphologies. The inset on the upper right-hand corner of the upper left-hand image is a selected-area electron diffraction pattern obtained from the particles within the dashed circle indicated on the image, with *d*-spacings of 1.9, 2.5 and 4.8 Å, which correspond to the diffraction patterns of the magnetite {420}, {311} and {111} planes, respectively.

about 200 times weaker than magnetite (Dunlop and Özdemir, 1997). This indicates that the mass concentration of hematite in the studied sediments is approximately equivalent to the magnetite concentration.

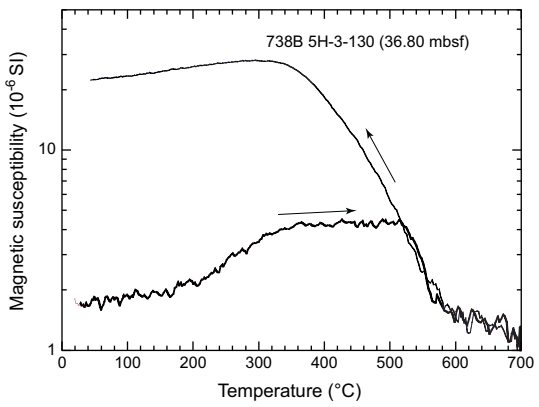

Fig. 5. Temperature-dependent susceptibility measurements for a sample from 36.80 mbsf (738B-5H-3-130 cm). This sample contains both magnetite (sharp decline in susceptibility to 580 °C) and hematite (persistent signal that does not disappear until 680 °C). The magnetization of hematite is ~200 times weaker than magnetite, which indicates a significant absolute concentration of hematite. The increased susceptibility during the cooling cycle indicates that the sample has undergone thermal alteration during heating.

4. Discussion

4.1. Diagenetic influence on magnetic properties?

The major change in IRM at 42 mbsf is the most striking down-hole magnetic change in the studied portion of Hole 738B (Fig. 8b). There are no significant lithological variations in the studied core interval, so it is important to consider whether the marked down-hole decrease in magnetization could have resulted from diagenetic magnetite dissolution (e.g., Channell and Hawthorne, 1990; Karlin, 1990a, b; Karlin and Levi, 1983; Rowan et al., 2009; Tarduno, 1994). Sedimentary manganese enrichments above crustal values and undetectable uranium contents both indicate that bottom waters were oxygenated throughout deposition (Faul and Delaney, 2010). The nearly complete absence of organic carbon in sediments at Site 738 places a severe limitation on microbial activity below the seafloor and pore water sulphate decreases from sea water values of ~28 mmol by about ~20% in the upper 50 mbsf and then remains essentially constant at ~22–24 mmol (Chambers and Cranston, 1991). These factors indicate that the sediments at Site 738 experienced suboxic but not anoxic conditions, and that the marked down-hole IRM decrease at 42 mbsf (Fig. 8b) is not due to reductive dissolution of magnetite. Preservation of bacterial magnetite is possible because diagenetic conditions never became anoxic. While the magnetic signal below 42 mbsf in Hole 738B is too weak to enable robust FORC and IRM acquisition measurements, noisy EPR results (not shown)

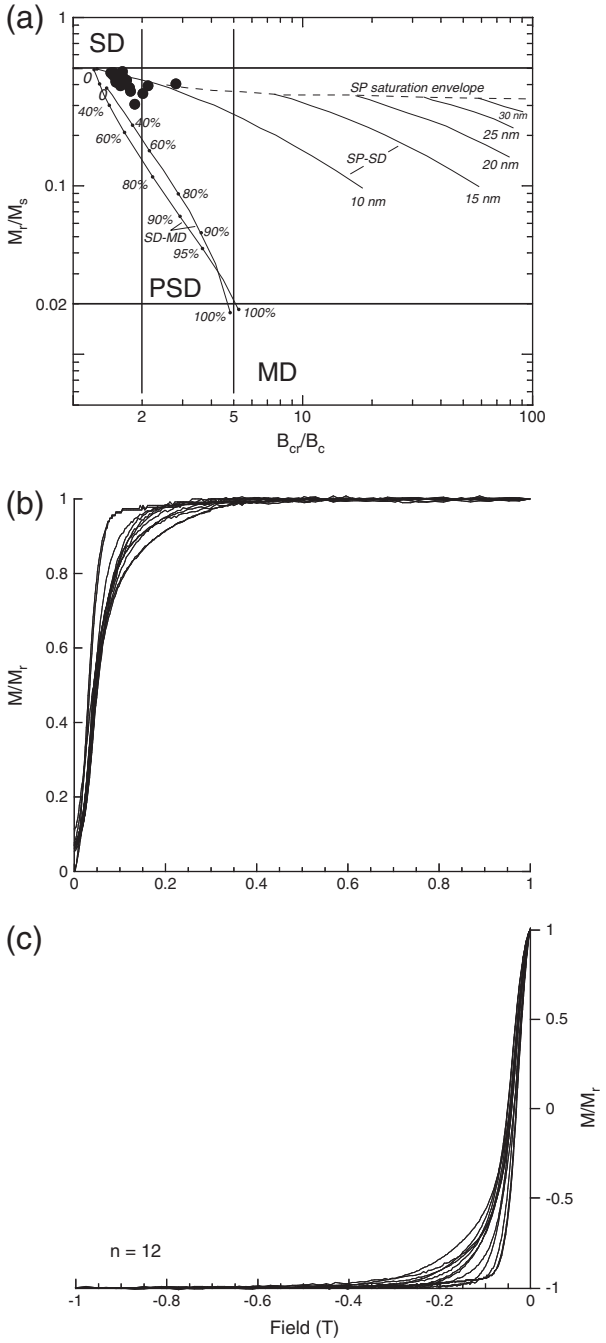

Fig. 6. (a) Magnetic hysteresis parameters represented on a plot of M_r/M_s versus B_{cr}/B_c (Day et al., 1977) for samples from ODP Hole 738B. The data fields represent areas expected for single domain (SD), pseudo-single domain (PSD), and multi-domain (MD) (titano-) magnetite particles. The data fall close to, but just outside, the SD field for magnetite, as would be expected for mixtures of SD magnetite magnetosomes and coarser aeolian particles. The curves represent theoretical mixing lines for SD–MD and SP–SD mixtures (where the grain size in nm represents the SP grain size; after Dunlop, 2002). (b) IRM acquisition and (c) backfield demagnetization curves for 12 studied samples from ODP Hole 738B. See text for discussion.

contain a weak dual peak at low fields that indicates the presence of a small concentration of fossil magnetosomes in this interval. Magnetotactic bacterial populations must have therefore persisted throughout the studied sediments, but their populations evidently increased significantly at 42 mbsf.

While it is evident that diagenetic conditions never became anoxic, magnetotactic bacteria require microaerobic conditions in chemically stratified environments. The suboxic conditions inferred for ODP Site 738 by Chambers and Cranston (1991) will therefore have given rise to iron reduction that liberated bioavailable dissolved iron for magnetosome growth. Sufficient organic carbon must also have been present in the sediments to give rise to suboxic conditions and to nourish microbial populations. Expanded diagenetic zonations, in which iron reduction but no sulphate reduction occurs, are reported in organic-carbon-poor pelagic carbonate environments (e.g., Chambers and Cranston, 1991; Tarduno, 1994), which appear to be necessary to explain both the presence of magnetotactic bacteria and the preservation of magnetofossils at Site 738. However, how were iron and organic carbon supplied to this open-ocean environment that appears to have been iron-limited and low in organic carbon?

4.2. Nutrient limitations for magnetotactic bacteria

Calcareous nannofossil data indicate that oligotrophic conditions dominated the interval from 86 to 43 mbsf at ODP Hole 738B (Fig. 8c), with nutrient-depleted surface waters. From 43 mbsf to the top of the studied section, eutrophic conditions prevailed. The switch from oligotrophic to eutrophic conditions coincides with increased hematite concentrations (Fig. 8a), but precedes by ~1 m a marked IRM increase that indicates a major increase in magnetofossil abundance (Fig. 8b). We interpret the increased hematite concentration to reflect a major influx of aeolian dust, probably sourced from Antarctica (Ehrmann and Mackensen, 1992), which would have brought nutrients, including iron, to the photic zone and increased primary productivity. Iron is an essential limiting micronutrient for phytoplankton growth in high-nutrient low-chlorophyll waters, where iron inputs associated with aeolian dust fluxes play an important role in stimulating primary productivity (e.g., Boyd and Ellwood, 2010; Jickells et al., 2005; Martin et al., 1991). The relative insolubility of iron means that dissolved iron concentrations in the open ocean are usually below 1 nmol l^{-1} (and are often much lower) unless they are enhanced by lateral advection, hydrothermal supply or atmospheric deposition (e.g., Boyd and Ellwood, 2010; Morel and Price, 2003). Lateral advection of iron from ocean islands, such as Kerguelen and Crozet islands in the Southern Ocean, produces natural iron fertilization that can stimulate large phytoplankton blooms (e.g., Blain et al., 2001; Pollard et al., 2007). Likewise, deposition of aeolian dust onto the surface ocean can result in dissolution of the most labile iron, which increases the availability of dissolved iron to nanomolar levels and can provide sufficient iron to enhance phytoplankton productivity in oligotrophic waters (e.g., Bonnet and Guieu, 2004). Other possible causes of increased nutrient delivery to Site 738 include enhanced vertical mixing due to internal wave activity (Blain et al., 2007) or upwelling of relatively nutrient-enriched waters (Faul and Delaney, 2010), but the coincidence between increased eutrophic nannofossil taxa and enhanced aeolian dust input suggests that natural aeolian iron fertilization played a significant role. Crucially, enhanced dust deposition and primary productivity would have had two benefits for magnetotactic bacteria at the seafloor, as outlined below.

First, increased dust supply would have provided a source of iron under iron-reducing sedimentary conditions that would be available for magnetosome biomineralization. It is important to consider the potential sources and quantities of iron needed by magnetotactic bacteria for magnetosome biomineralization. The iron content of magnetotactic bacteria can exceed 2% of their dry weight (Blakemore et al., 1979). Schüler and Baeuerlein (1996) demonstrated that for freshwater *Magnetospirillum gryphiswaldense*, magnetosome biomineralization is limited by availability of dissolved iron (uptake of both Fe^{2+} and Fe^{3+} is possible). Magnetosome concentrations were observed to increase markedly at dissolved iron concentrations of 1 μmol l^{-1}, with biomineralization close to saturation at iron concentrations of 10–20 μmol l^{-1}. Flies et al. (2005) also reported the presence of magnetotactic bacteria in laboratory freshwater sediment microcosms with dissolved Fe^{2+} concentrations of 6–60 μmol l^{-1}. These concentrations are orders of magnitude higher than the nmol l^{-1} concentrations of iron in modern

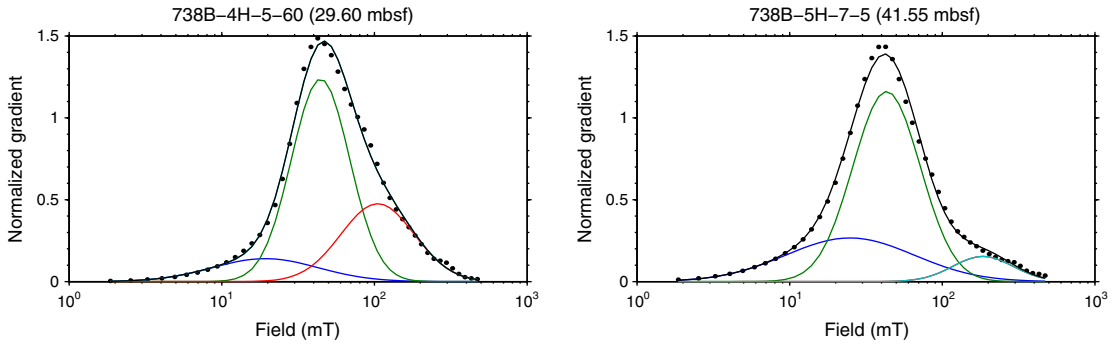

Fig. 7. Results of IRM component analysis (Heslop et al., 2002). The derivative of the IRM acquisition curve is plotted as solid circles. The fitted IRM components are indicated in different colours and the sum of the three fitted components is plotted in black to enable visual comparison of the quality of the fit to the measured data. The data are normalized so that the integral of the derivative is unity. The dominant component has a narrow distribution and is due to biogenic magnetite (i.e., the "biogenic soft" component of Egli (2004b)). The broader low- and high-coercivity distributions are due to detrital (probably aeolian) magnetite and hematite, respectively. The high coercivity component has variable coercivities. A list of relevant parameters associated with each component is given in Table 2. (For interpretation of the references to colour in this figure legend, the reader is referred to the web version of this article.)

deep waters (Boyd and Ellwood, 2010; Morel and Price, 2003). Thus, while dissolution of aeolian particulates is clearly important for fertilizing primary productivity, the nanomolar iron concentrations produced (e.g., Bonnet and Guieu, 2004) are only adequate for uptake by marine phytoplankton, which have highly efficient iron uptake systems. Such low dissolved iron concentrations are unlikely to be able to sustain a thriving population of magnetotactic bacteria, as indicated by our observations of extremely small concentrations of magnetofossils in the oligotrophic environment below 42 mbsf at Hole 738B. In contrast, suboxic iron-reducing diagenetic environments typically produce the micromolar concentrations of dissolved iron (e.g., Froelich et al., 1979) that are apparently needed for magnetosome biomineralization (Schüler

Table 2
Parameters associated with components identified from IRM unmixing analysis.

Sample	Component 1	Component 2	Component 3	Component 4
	M_r (Am^2/kg)	M_r (Am^2/kg)	M_r (Am^2/kg)	M_r (Am^2/kg)
738B-3H-5-115	3.48E+02	1.01E+03	NA	4.33E+01
738B-3H-6-120	2.42E+02	9.13E+02	NA	5.13E+00
738B-4H-2-127	1.35E+02	4.56E+02	2.40E+02	NA
738B-4H-3-58	8.53E+01	3.44E+02	1.54E+02	NA
738B-4H-4-85	9.24E+01	4.08E+02	1.97E+02	NA
738B-4H-5-60	8.99E+01	4.37E+02	2.12E+02	NA
738B-4H-6-130	1.24E+02	6.32E+02	3.29E+02	NA
738B-5H-1-130	3.96E+01	2.13E+02	1.32E+02	NA
738B-5H-3-130	4.99E+01	3.46E+02	4.19E+01	NA
738B-5H-4-132	5.03E+01	1.60E+02	NA	2.35E-01
738B-5H-7-5	1.19E+02	2.72E+02	NA	3.22E+01
	$B_{1/2}$ (mT)	$B_{1/2}$ (mT)	$B_{1/2}$ (mT)	$B_{1/2}$ (mT)
738B-3H-5-115	13.5	35.5	NA	302.0
738B-3H-6-120	15.1	40.7	NA	346.7
738B-4H-2-127	16.2	39.8	128.8	NA
738B-4H-3-58	17.8	42.7	109.7	NA
738B-4H-4-85	17.8	43.7	107.2	NA
738B-4H-5-60	19.1	44.7	104.7	NA
738B-4H-6-130	20.4	44.7	104.7	NA
738B-5H-1-130	22.4	45.7	102.3	NA
738B-5H-3-130	17.8	46.8	125.9	NA
738B-5H-4-132	20.9	42.7	NA	354.8
738B-5H-7-5	25.1	43.7	NA	186.2
	DP (log_{10} mT)	DP (log_{10} mT)	DP (log_{10} mT)	DP (log_{10} mT)
738B-3H-5-115	0.33	0.19	NA	0.11
738B-3H-6-120	0.34	0.19	NA	0.07
738B-4H-2-127	0.37	0.23	0.26	NA
738B-4H-3-58	0.36	0.20	0.26	NA
738B-4H-4-85	0.35	0.20	0.25	NA
738B-4H-5-60	0.35	0.19	0.24	NA
738B-4H-6-130	0.34	0.18	0.23	NA
738B-5H-1-130	0.32	0.17	0.22	NA
738B-5H-3-130	0.33	0.19	0.14	NA
738B-5H-4-132	0.39	0.20	NA	0.03
738B-5H-7-5	0.42	0.22	NA	0.20

NA = not applicable (i.e., this component is not present in the sample). $B_{1/2}$ is the coercivity associated with the peak of the fitted component in Fig. 7; DP is the dispersion of the distribution (see Heslop et al. (2002) for details).

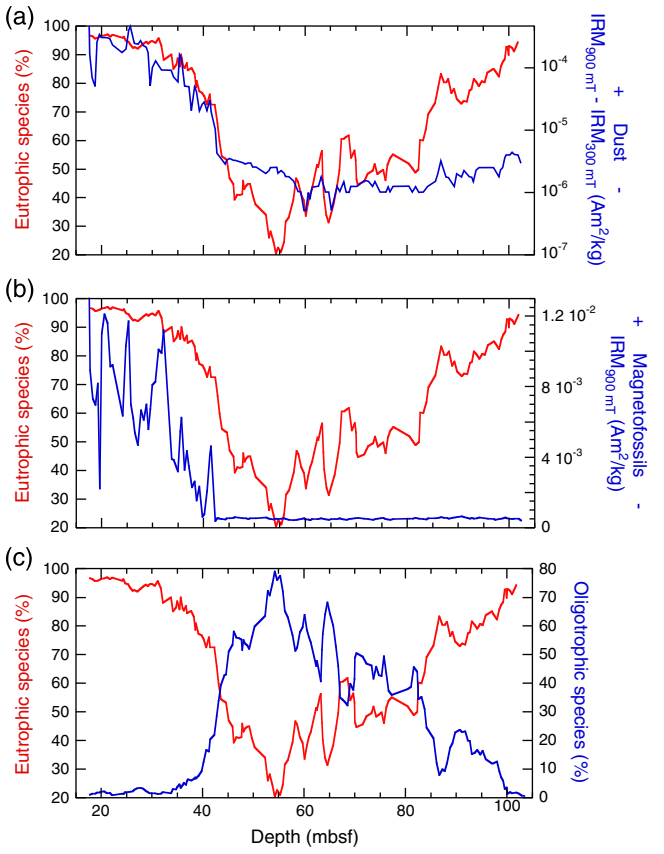

Fig. 8. Magnetic and productivity proxies for ODP Hole 738B. (a) Variations in hematite content (proxy for aeolian dust) and eutrophic nannofossil taxa in ODP Hole 738B. The increase in eutrophic taxa coincides with an increase in aeolian dust, which suggests that iron fertilization by enhanced delivery of dust to Hole 738B is responsible for the observed increase in primary productivity. (b) Variations in IRM (proxy for magnetite magnetofossil content) and eutrophic nannofossil taxa in ODP Hole 738B. The delayed bacterial magnetite response to increased productivity is interpreted to reflect a delay in export of labile organic carbon to the seafloor (see text). (c) Variations in oligotrophic and eutrophic nannofossil taxa in ODP Hole 738B, which provide a measure of nutrient availability in the surface waters above the southern Kerguelen Plateau throughout the studied time interval.

and Baeuerlein, 1996). The iron that was dissolved and made bioavailable to magnetotactic bacteria would have come from the most labile minerals under iron reducing conditions (i.e., hydrous ferric oxide and lepidocrocite; Poulton et al., 2004). Our results indicate that the less reactive magnetite and hematite (Poulton et al., 2004) evidently did not undergo dissolution. It therefore appears that an increased supply of reducible iron, which was delivered via increased aeolian sediment input, and that was made bioavailable by suboxic diagenetic iron reduction, was needed at ODP Site 738 to provide the necessary iron for magnetosome biomineralization. Our observations provide strong palaeoenvironmental support for the availability of dissolved iron as a major limiting factor for magnetotactic bacteria, as has been demonstrated in the laboratory by Schüler and Baeuerlein (1996).

Second, increased primary productivity is likely to have increased delivery of organic matter to the seafloor that would have been necessary for magnetotactic bacterial metabolism. This conclusion is not immediately obvious because the efficiency of the biological pump in exporting the carbon fixed by phytoplankton blooms is low and the degree of seafloor sequestration of such carbon is poorly quantified (e.g., Boyd et al., 2004; Buesseler et al., 2004; Pollard et al., 2007). Although carbon export is inefficient, Blain et al. (2007) and Pollard et al. (2007) demonstrated that natural iron fertilization in the Southern Ocean directly enhances carbon export to the seafloor. Given the evidence summarized above for suboxic diagenetic conditions at ODP Site 738 (Chambers and Cranston, 1991), it is highly likely that the increased primary productivity indicated by the increase in eutrophic nannofossils at 43 mbsf resulted in increased organic carbon flux to the seafloor. The increased magnetofossil concentration at 42 mbsf provides further circumstantial evidence for our interpretation because, as argued above, their increased presence requires iron release under suboxic diagenetic conditions; suboxic conditions in turn require organic carbon supply (cf. Froelich et al., 1979). Based on the age model of Bohaty et al. (in prep.), a delay of ~120 kyr between the increase in hematite content (at 43 mbsf) and the major increase in magnetofossil preservation (at 42 mbsf; Fig. 8a, b) indicates a time lag between stimulation of productivity of eutrophic nannofossil taxa and delivery of sufficient iron and labile organic carbon to the seafloor to stimulate enhancement of magnetotactic bacterial populations. Negligible remaining organic carbon concentrations in the sediments suggest that microbial demand consumed all labile organic carbon, which can explain the lag between organic supply and magnetotactic bacterial enhancement.

While iron is an important limiting micronutrient for primary producers in oligotrophic oceanic settings, it is only one of several limiting nutrients and the interplay among various nutrients is complex and incompletely understood (e.g., Morel and Price, 2003). For example, there are coincident variations between iron supply (dust) and a decline in eutrophic species between 103 and 55 mbsf; however, the relative amplitudes of these variations are not the same as for the interval from 55 to 16 mbsf (Fig. 8a). This non-linear relationship should not be surprising in light of the complexities of nutrient limitations (e.g., Bailey et al., 2011; Morel and Price, 2003). Villa et al. (2008) also reported significant sea surface temperature variations in the interval between 38 and 36 Ma at ODP Site 748 on Kerguelen Plateau. Such variations can be as important as nutrient influences on nannofossil assemblages, therefore sea surface temperature variations are also a likely contributor to the observed non-linear relationship between iron fertilization and nannofossil trophic state. Nevertheless, the documented relationship between iron fertilization, nannoplankton productivity and magnetotactic bacterial productivity at Site 738 indicate that iron and organic carbon supply to the seafloor are important limiting factors for magnetotactic bacteria in oligotrophic marine settings.

4.3. Magnetofossils as recorders of palaeoecological information

While there is considerable scope for exploring the use of magnetofossils as potential biogeochemical indicators (e.g., Kopp and Kirschvink, 2008), relatively few studies have provided strong constraints from magnetofossil records about the interplay between nutrient limitations, climate or organic carbon flux and palaeoproductivity in deep-sea environments (e.g., Dinarès-Turell et al., 2003; Hesse, 1994; Lean and McCave, 1998; Tarduno, 1994; Tarduno and Wilkison, 1996; Yamazaki, 2009; Yamazaki and Kawahata, 1998). Magnetofossils have been shown in some settings to be sensitive to glacial–interglacial variations, with higher magnetofossil abundances reported in interglacials compared to glacials, although the precise relationship between palaeoecology and climate has remained elusive (Dinarès-Turell et al., 2003; Hesse, 1994; Lean and McCave, 1998). Yamazaki and Kawahata (1998) argued that magnetosome morphology is an indicator of sedimentary palaeo-oxygenation state, with isotropic crystals dominating in relatively oxidized settings with lower organic carbon fluxes and anisotropic crystals dominating in relatively reduced settings with higher organic carbon fluxes. Like Hesse (1994), we observe the simultaneous presence of multiple magnetotactic bacterial species with variable magnetosome morphologies (Fig. 4), but we have not been able to obtain a large enough set of magnetic extracts or sufficiently representative extracts to enable quantitative comparison of the range of magnetofossil morphologies in the studied Hole 738B sediments. Furthermore, lack of information about organic carbon fluxes in the studied sediments precludes comparison with the inferences of Yamazaki and Kawahata (1998). However, variable coercivity spectra from FORC distributions (Fig. 2n) and IRM acquisition results (Fig. 7) suggest stratigraphic variations in the balance between different magnetosome morphologies. This variability could have palaeoecological significance.

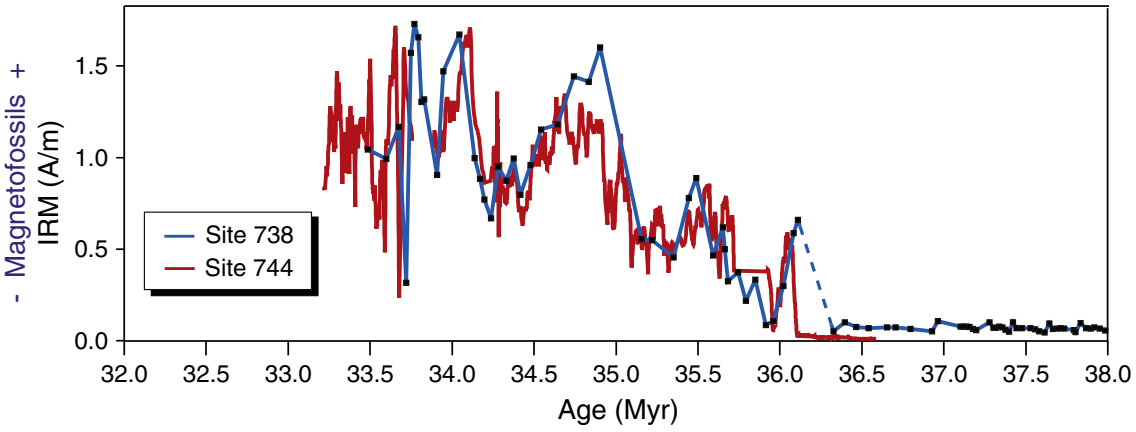

Fig. 9. Coeval variations in magnetite magnetofossil abundances across the southern Kerguelen Plateau. The coherence of the magnetofossil signature across the southern Kerguelen Plateau, as indicated by IRM, indicates a regional rather than a local magnetotactic bacterial productivity signature. The age model is from Bohaty et al. (in preparation).

Regardless of the above possibilities, we observe coeval, coherent variations in IRM (Fig. 9) and eutrophic nannofossil taxa across the southern Kerguelen Plateau. Regional synchroneity of the magnetic and nannofossil productivity records further indicate that these processes are not isolated, but that they represent large-scale variations across the southern Kerguelen Plateau. Persico and Villa (2004) observed similar nannofossil palaeoecological variations across the Southern Ocean (from Kerguelen Plateau to Maud Rise). It is therefore possible that a magnetofossil-based palaeoproductivity signal could be recorded in Eocene sediments from the wider Southern Ocean. This possibility remains to be tested, but the potential of using sediment magnetization as a palaeo-productivity proxy for magnetotactic bacteria in pelagic carbonates from oligotrophic settings merits further investigation.

While we appear to have documented a magnetofossil signature that reflects Southern Ocean palaeoproductivity, this relationship would not be expected in settings with higher organic carbon fluxes. Tarduno (1992) observed cycles with high and low magnetic mineral concentrations, respectively, in Cretaceous pelagic carbonates from Italy. He inferred that this pattern is due to 100-kyr palaeoproductivity cycles with intervals of greater magnetite dissolution corresponding to higher sedimentary organic carbon contents that occurred between more strongly magnetized intervals with lower inferred organic carbon flux and better magnetite preservation. This interpretation could be valid, but the data of Tarduno (1992) do not preclude the relationship with palaeoproductivity observed in this study. Regardless, there are well-documented cases in which our observed relationship does not hold. For example, Tarduno (1994) reported changes in magnetic properties in pelagic carbonates from the western equatorial Pacific Ocean that clearly relate to glacial–interglacial change in palaeoproductivity. In sediments with higher organic carbon fluxes, the modern sedimentary redox boundaries occur at shallower depths than for those with lower organic carbon fluxes, with increased productivity causing increased magnetite dissolution. Organic carbon supply is therefore important for driving both reductive dissolution (e.g., Karlin and Levi, 1983; Tarduno, 1994) and magnetofossil abundance (e.g., Yamazaki and Kawahata, 1998). Variations in palaeoproductivity can therefore give rise to cycles with strong and weak magnetic properties, respectively, associated with cycles of both non-steady state diagenesis in pelagic carbonates (e.g., Tarduno, 1992, 1994) and other deep-sea sediments (e.g., Larrasoaña et al., 2003), but also in pelagic carbonates that have not evidently undergone reductive diagenesis (e.g., Jovane et al., 2004, 2007; Florindo and Roberts, 2005). It remains to be determined where the critical balance lies between the importance of palaeoproductivity variations and diagenetic destruction of the palaeomagnetic record versus palaeoproductivity variations and stimulation of an enhanced palaeomagnetic record through increased magnetofossil abundance. Future work is needed to test where this balance lies in the geological record and how these processes contribute to the magnetic properties of pelagic carbonates.

4.4. Magnetofossils as recorders of palaeomagnetic information

Magnetotactic bacteria produce SD particles that are ideal for recording palaeomagnetic signals. This is evident in the high palaeomagnetic stability and clearly defined magnetic polarity zonations of Eocene-Oligocene pelagic carbonate sediments from the South Atlantic and Southern Oceans (e.g., Channell et al., 2003; Florindo and Roberts, 2005; Roberts et al., 2003; Tauxe and Hartl, 1997), which have magnetic properties that are consistent with those reported here. The zone with low IRM intensity below 36.2 Ma in Hole 744A (Fig. 9), which has low concentrations of magnetofossils, does not contain a reliable palaeomagnetic record, in contrast to that from the overlying, more strongly magnetized sediments (Roberts et al., 2003). Magnetofossil abundance is therefore an important determinant of the palaeomagnetic recording fidelity of such sediments.

Despite the palaeomagnetic stability of the studied sediments, it is important to consider the depth at which the palaeomagnetic signal is recorded/locked in within these pelagic carbonates. Magnetotactic bacteria have been reported to live within the sediment and are restricted to chemical gradients in narrow intervals at or below the maximum depth of penetration of oxygen and nitrate (Flies et al., 2005; Petermann and Bleil, 1993; Schüler and Baeuerlein, 1998). In many sediments, the depth of this chemical interface is shallow. Any magnetization recorded by such magnetofossils will be equivalent to a syn-depositional paleomagnetic signal. However, Tarduno and Wilkison (1996) and Tarduno et al. (1998) reported that the depth to this chemical interface varies with organic carbon flux, with the interface occurring at greater depths in sediments with lower organic carbon contents. In such settings, magnetofossils are argued to give rise to palaeomagnetic signals that are delayed with respect to the age of the sediment in which they occur by periods between <40 kyr and up to 425 kyr (Tarduno et al., 1998; Tarduno and Wilkison, 1996). In contrast, Yamazaki and Sølheid (2011) did not observe any significant apparent delays in remanence acquisition in their relative geomagnetic palaeointensity records across the iron redox boundary in nearby sites on the Ontong-Java Plateau. Abrajevitch and Kodama (2009) reported biogeochemical remanent magnetizations across the Cretaceous-Tertiary boundary in the hole adjacent to that studied here (i.e., ODP Hole 738C) and argued that it provides the dominant remanence acquisition process in these sediments. Increased recognition of such biogeochemical remanences is likely to become more widespread with routine use of FORC diagrams and EPR analyses in association with palaeomagnetic studies of such sediments. The crucial question in terms of palaeomagnetic investigations therefore concerns the depth at which the palaeomagnetic signal is locked in. The possibility of large delays in magnetization acquisition is important for interpretation of the chronology of such sediments. It is difficult to constrain precisely the depth at which the palaeomagnetic signal is locked in within the studied sediments. The fidelity of the palaeomagnetic record and good correlation between ODP sites 738 and 744 (Fig. 9), which is based on magnetostratigraphy, suggests that the palaeomagnetic signal was acquired at shallow depths, but deeper lock-in is not conclusively precluded by this observation. Further work is needed from a range of settings to better understand the timing of biogeochemical remanence acquisition associated with magnetofossils.

5. Conclusions

Our results suggest several conclusions. First, similar approaches to those that we have employed should enable better documentation of the preservation of magnetite magnetofossils in the geological record. We expect such approaches to extend considerably the range of pre-Quaternary sites from which magnetofossils have been documented (cf. Kopp and Kirschvink, 2008). For example, recent studies of other age intervals at ODP Site 738 provide similar indications of the widespread presence of magnetofossils in these pelagic carbonate sediments (e.g., Abrajevitch and Kodama, 2009 (Creteaceous-Tertiary boundary); Larrasoaña et al., in prep. (Palaeocene-Eocene Thermal Maximum)). This will improve our understanding of the real importance of bacterial magnetite in palaeomagnetic records and as palaeoenvironmental indicators. Second, iron and organic carbon are important limiting factors for magnetotactic bacterial metabolism; iron fertilization via increased dust flux to oligotrophic waters provides a mechanism to both supply reactive iron and to increase organic carbon export to the sea floor. Third, while cycles of strong and weak magnetic properties have been associated with cycles of non-steady state diagenesis associated with palaeoproductivity variations in pelagic carbonates (e.g., Tarduno, 1992, 1994) and other deep-sea sediments (e.g., Larrasoaña et al., 2003), variations between strongly and weakly magnetic intervals are also often documented in pelagic carbonates that have not evidently undergone reductive diagenesis (e.g., Florindo and Roberts, 2005;

Jovane et al., 2004). Organic carbon supply is important for driving both reductive dissolution (e.g., Karlin and Levi, 1983; Tarduno, 1994) and magnetofossil abundance (e.g., Yamazaki and Kawahata, 1998). It remains to be determined where the critical balance lies between the importance of palaeoproductivity variations and diagenetic destruction of the palaeomagnetic record versus palaeoproductivity variations and stimulation of an enhanced palaeomagnetic record through increased magnetofossil abundance. Future work should test where the balance lies between the processes described here in the geological record and how they contribute to the magnetic properties of pelagic carbonates. Finally, while multiple factors influence nutrient limitations and the productivity of marine organisms, testing the use of sediment magnetization as a palaeoproductivity proxy for magnetotactic bacteria in pelagic carbonates merits further investigation.

Acknowledgements

We thank the Integrated Ocean Drilling Program (IODP) for providing access to the studied cores. The IODP was sponsored by the U.S. National Science Foundation (NSF) and participating countries under the management of Joint Oceanographic Institutions (JOI), Inc. Shane Paxton provided assistance with magnetic mineral extraction. TEM access was obtained through the Centre for Advanced Microscopy at the ANU, which is a node of the Australian Microscopy and Microanalysis Research Facility. We thank J. Wolowska for technical assistance with EPR measurements, which were made at the EPR National Service Centre at the University of Manchester, which is funded by the UK Engineering and Physical Sciences Research Council. We are grateful to Michael Winklhofer, John Tarduno and an anonymous reviewer for comments that helped to improve this paper, and to Peter deMenocal for editorial handling. Parts of this work benefitted from funding from the UK Natural Environment Research Council grant NE/G003319/1 to APR and from the Istituto Nazionale di Geofisica e Vulcanologia, and the Italian National Antarctic Research Program (PNRA) to FF and GV.

References

Abrajevitch, A., Kodama, K., 2009. Biochemical vs. detrital mechanism of remanence acquisition in marine carbonates: a lesson from the K-T boundary interval. Earth Planet. Sci. Lett. 286, 269–277.

Bailey, I., Liu, Q.S., Swann, G.E.A., Jiang, Z.X., Sun, Y.B., Zhao, X., Roberts, A.P., 2011. Iron fertilisation and biogeochemical cycles in the sub-Arctic northwest Pacific during the late Pliocene intensification of northern hemisphere glaciation. Earth Planet. Sci. Lett. 307, 253–265.

Bazylinski, D.A., Frankel, R.B., 2004. Magnetosome formation in prokaryotes. Nat. Rev. Microbiol. 2, 217–230.

Bazylinski, D.A., Heywood, B.R., Mann, S., Frankel, R.B., 1993. Fe_3O_4 and Fe_3S_4 in a bacterium. Nature 366, 218.

Bazylinski, D.A., Frankel, R.B., Konhauser, K.O., 2007. Modes of biomineralization of magnetite by microbes. Geomicrobiol. J. 24, 465–475.

Blain, S., et al., 2001. A biogeochemical study of the island mass effect in the context of the iron hypothesis: Kerguelen Islands, Southern Ocean. Deep-Sea Res. I 48, 163–187.

Blain, S., et al., 2007. Effect of natural iron fertilization on carbon sequestration in the Southern Ocean. Nature 446, 1070–1074.

Blakemore, R.P., Maratea, D., Wolfe, R.S., 1979. Isolation and pure culture of a freshwater magnetic spirillum in chemically defined media. J. Bacteriol. 140, 720–729.

Blakemore, R.P., Short, K.A., Bazylinski, D.A., Rosenblatt, C., Frankel, R.B., 1985. Microaerobic conditions are required for magnetite formation within *Aquaspirillum magnetotacticum*. Geomicrobiol. J. 4, 53–71.

Bonnet, S., Guieu, C., 2004. Dissolution of atmospheric iron in seawater. Geophys. Res. Lett. 31, L03303. doi:10.1029/2003GL018423.

Boughriet, A., Ouddane, B., Wartel, M., 1992. Electron spin resonance investigations of Mn compounds and free radicals in particles from the Seine River and its estuary. Mar. Chem. 37, 149–169.

Boyd, P.W., Ellwood, M.J., 2010. The biogeochemical cycle of iron in the ocean. Nat. Geosci. 3, 675–682.

Boyd, P.W., et al., 2004. The decline and fate of an iron-induced subarctic phytoplankton bloom. Nature 428, 549–553.

Buesseler, K.O., Andrews, J.E., Pike, S.M., Charette, M.A., 2004. The effects of iron fertilization on carbon sequestration in the Southern Ocean. Science 304, 414–417.

Chambers, S.R., Cranston, R.E., 1991. Interstitial-water geochemistry of Kerguelen Plateau sediments. Proc. ODP Sci. Res. 119, 347–374.

Channell, J.E.T., Hawthorne, T., 1990. Progressive dissolution of titanomagnetites at ODP Site 653 (Tyrrhenian Sea). Earth Planet. Sci. Lett. 96, 469–480.

Channell, J.E.T., Galeotti, S., Martin, E.E., Billups, K., Scher, H.D., Stoner, J.S., 2003. Eocene to Miocene magnetostratigraphy, biostratigraphy, and chemostratigraphy at ODP Site 1090 (sub-Antarctic South Atlantic). Geol. Soc. Am. Bull. 115, 607–623.

Charilaou, M., Winklhofer, M., Gehring, A.U., 2011. Simulation of ferromagnetic resonance spectra of linear chains of magnetite nanocrystals. J. Appl. Phys. 109, 093903. doi:10.1063/1.3581103.

Day, R., Fuller, M., Schmidt, V.A., 1977. Hysteresis properties of titanomagnetites: grain size and composition dependence. Phys. Earth Planet. Inter. 13, 260–266.

de Boor, C., 1994. A Practical Guide to Splines (Applied Mathematical Sciences). Springer.

Dinarès-Turell, J., Hoogakker, B.A.A., Roberts, A.P., Rohling, E.J., Sagnotti, L., 2003. Quaternary climatic control of biogenic magnetite production and eolian dust input in cores from the Mediterranean Sea. Palaeogeogr. Palaeoclimatol. Palaeoecol. 190, 195–209.

Dunlop, D.J., 2002. Theory and application of the Day plot (M_{rs}/M_s versus H_{cr}/H_c) 1. Theoretical curves and tests using titanomagnetite data. J. Geophys. Res. 107 (B3), 2056. doi:10.1029/2001JB000486.

Dunlop, D.J., Özdemir, Ö., 1997. Rock Magnetism, Fundamentals and Frontiers. Cambridge University Press, Cambridge.

Egli, R., 2004a. Characterization of individual rock magnetic components by analysis of remanence curves, 1. Unmixing natural sediments. Stud. Geophys. Geod. 48, 391–446.

Egli, R., 2004b. Characterization of individual rock magnetic components by analysis of remanence curves, 2. Fundamental properties of coercivity distributions. Phys. Chem. Earth 29, 851–867.

Egli, R., Chen, A.P., Winklhofer, M., Kodama, K.P., Horng, C.S., 2010. Detection of noninteracting single domain particles using first-order reversal curve diagrams. Geochem. Geophys. Geosyst. 11, Q01Z11. doi:10.1029/2009GC002916.

Ehrmann, W.U., Mackensen, A., 1992. Sedimentological evidence for the formation of an East Antarctic ice sheet in Eocene/Oligocene time. Palaeogeogr. Palaeoclimatol. Palaeoecol. 93, 85–112.

Eldholm, O., Coffin, M.F., 2000. Large igneous provinces and plate tectonics. In: Richards, M., Gordon, A.R.G., van der Hilst, R.D. (Eds.), The History and Dynamics of Global Plate Motions. American Geophysical Union, Washington, D.C, pp. 309–326.

Faivre, D., Schüler, D., 2008. Magnetotactic bacteria and magnetosomes. Chem. Rev. 108, 4875–4898.

Faul, K.L., Delaney, M.L., 2010. A comparison of early Paleogene export productivity and organic carbon burial flux for Maud Rise, Weddell Sea, and Kerguelen Plateau, south Indian Ocean. Paleoceanography 25, PA3214. doi:10.1029/2009PA001916.

Fischer, H., Mastrogiacomo, G., Löffler, J.F., Warthmann, R.J., Weidler, P.G., Gehring, A.U., 2008. Ferromagnetic resonance and magnetic characteristics of intact magnetosome chains in *Magnetospirillum gryphiswaldense*. Earth Planet. Sci. Lett. 270, 200–208.

Flies, C.B., Jonkers, H.M., de Beer, D., Bosselmann, K., Böttcher, M.E., Schüler, D., 2005. Diversity and vertical distribution of magnetotactic bacteria along chemical gradients in freshwater microcosms. FEMS Microbiol. Ecol. 52, 185–195.

Florindo, F., Roberts, A.P., 2005. Eocene-Oligocene magnetobiostratigraphy of ODP sites 689 and 690, Maud Rise, Weddell Sea, Antarctica. Geol. Soc. Am. Bull. 117, 46–66.

Froelich, P.N., Klinkhammer, G.P., Bender, M.L., Luedtke, N.A., Heath, G.R., Cullen, D., Dauphin, P., Hammond, D., Hartman, B., Maynard, V., 1979. Early oxidation of organic matter in pelagic sediments of the eastern equatorial Atlantic: suboxic diagenesis. Geochim. Cosmochim. Acta 43, 1075–1090.

Heslop, D., Dekkers, M.J., Kruiver, P.P., van Oorschot, I.H.M., 2002. Analysis of isothermal remanent magnetisation acquisition curves using the expectation–maximisation algorithm. Geophys. J. Int. 148, 58–64.

Hesse, P.P., 1994. Evidence for bacterial palaeoecological origin of mineral magnetic cycles in oxic and sub-oxic Tasman Sea sediments. Mar. Geol. 117, 1–17.

Housen, B.A., Moskowitz, B.M., 2006. Depth distribution of magnetofossils in near-surface sediments from the Blake/Bahama Outer Ridge, western North Atlantic Ocean, determined by low-temperature magnetism. J. Geophys. Res. 111, G01005. doi:10.1029/2005JG000068.

Jickells, T.D., An, Z.S., Anderson, K.K., Baker, A.R., Bergametti, G., Brooks, N., Cao, J.J., Boyd, P.W., Duce, R.A., Hunter, K.A., Kawahata, H., Kubilay, N., laRoche, J., Liss, P.S., Mahowald, N., Prospero, J.M., Ridgwell, A.J., Tegen, I., Torres, R., 2005. Global iron connections between desert dust, ocean biogeochemistry, and climate. Science 308, 67–71.

Jovane, L., Florindo, F., Dinarès-Turell, J., 2004. Environmental magnetic record of paleoclimate change from the Eocene-Oligocene stratotype section, Massignano, Italy. Geophys. Res. Lett. 31, L15601. doi:10.1029/2004GL020554.

Jovane, L., Florindo, F., Coccioni, R., Dinarès-Turell, J., Marsili, A., Monechi, S., Roberts, A.P., Sprovieri, M., 2007. The middle Eocene climatic optimum (MECO) event in the Contessa Highway section, Umbrian Apennines. Italy. Geol. Soc. Am. Bull. 119, 423–427.

Karlin, R., 1990a. Magnetite diagenesis in marine sediments from the Oregon continental margin. J. Geophys. Res. 95, 4405–4419.

Karlin, R., 1990b. Magnetic mineral diagenesis in suboxic sediments at Bettis site W-N, NE Pacific Ocean. J. Geophys. Res. 95, 4421–4436.

Karlin, R., Levi, S., 1983. Diagenesis of magnetic minerals in Recent haemipelagic sediments. Nature 303, 327–330.

Kirschvink, J.L., 1982. Paleomagnetic evidence for fossil biogenic magnetite in Western Crete. Earth Planet. Sci. Lett. 59, 388–392.

Kopp, R.E., Kirschvink, J.L., 2008. The identification and biogeochemical interpretation of fossil magnetotactic bacteria. Earth-Sci. Rev. 86, 42–61.

Kopp, R.E., Weiss, B.P., Maloof, A.C., Vali, H., Nash, C.Z., Kirschvink, J.L., 2006. Chains, clumps, and strings: magnetofossil taphonomy with ferromagnetic resonance spectroscopy. Earth Planet. Sci. Lett. 247, 10–25.

Larrasoaña, J.C., Roberts, A.P., Stoner, J.S., Richter, C., Wehausen, R., 2003. A new proxy for bottom-water ventilation based on diagenetically controlled magnetic properties of eastern Mediterranean sapropel-bearing sediments. Palaeogeogr. Palaeoclimatol. Palaeoecol. 190, 221–242.

Lawver, L.A., Gahagan, L.M., 2003. Evolution of Cenozoic gateways in the circum-Antarctic region. Palaeogeogr. Palaeoclimatol. Palaeoecol. 198, 11–37.

Lean, C.M.B., McCave, I.N., 1998. Glacial to interglacial mineral magnetic and palaeoceanographic changes at Chatham Rise, SW Pacific Ocean. Earth Planet. Sci. Lett. 163, 247–260.

Martin, J.H., Gordon, R.M., Fitzwater, S.E., 1991. The case for iron. Limnol. Oceanogr. 36, 1793–1802.

Morel, F.M.M., Price, N.M., 2003. The biogeochemical cycles of trace metals in the oceans. Science 300, 944–947.

Otamendi, A.M., Díaz, M., Costanzo-Álvarez, V., Aldana, M., Pilloud, A., 2006. EPR stratigraphy applied to the study of two marine sedimentary sections in southwestern Venezuela. Phys. Earth Planet. Inter. 154, 243–254.

Persico, D., Villa, G., 2004. Eocene-Oligocene calcareous nannofossils from Maud Rise and Kerguelen Plateau (Antarctica): paleoecological and paleoceanographic implications. Mar. Micropal. 52, 153–179.

Persico, D., Fioroni, C., Villa, G., 2011. A refined calcareous nannofossil biostratigraphy for the Middle Eocene-Early Oligocene Southern Ocean ODP sites. Palaeogeogr. Palaeoclimatol. Palaeoecol.. doi:10.1016/j.paleo.2011.05.017

Petermann, H., Bleil, U., 1993. Detection of live magnetotactic bacteria in South Atlantic deep-sea sediments. Earth Planet. Sci. Lett. 117, 223–228.

Petersen, N., von Dobeneck, T., Vali, H., 1986. Fossil bacterial magnetite in deep-sea sediments from the South Atlantic Ocean. Nature 320, 611–614.

Pike, C.R., Roberts, A.P., Verosub, K.L., 1999. Characterizing interactions in fine magnetic particle systems using first order reversal curves. J. Appl. Phys. 85, 6660–6667.

Pollard, R.T., et al., 2007. Southern Ocean deep-water carbon export enhanced by natural iron fertilization. Nature 457, 577–580.

Poulton, S.W., Krom, M.D., Raiswell, R., 2004. A revised scheme for the reactivity of iron (oxyhydr)oxide minerals towards dissolved sulfide. Geochim. Cosmochim. Acta 68, 3703–3715.

Roberts, A.P., Pike, C.R., Verosub, K.L., 2000. FORC diagrams: a new tool for characterizing the magnetic properties of natural samples. J. Geophys. Res. 105, 28461–28475.

Roberts, A.P., Bicknell, S., Byatt, J., Bohaty, S.M., Florindo, F., Harwood, D.M., 2003. Magnetostratigraphic calibration of Southern Ocean diatom biostratigraphic datums from the Eocene-Oligocene of Kerguelen Plateau (ODP sites 744 and 748). Palaeogeogr. Palaeoclimatol. Palaeoecol. 198, 145–168.

Robertson, D.J., France, D.E., 1994. Discrimination of remanence-carrying minerals in mixtures, using isothermal remanent magnetisation acquisition curves. Phys. Earth Planet. Inter. 84, 223–234.

Rowan, C.J., Roberts, A.P., Broadbent, T., 2009. Paleomagnetic smoothing and magnetic enhancement in marine sediments due to prolonged early diagenetic growth of greigite. Earth Planet. Sci. Lett. 277, 223–235.

Schüler, D., Baeuerlein, E., 1996. Iron-limited growth and kinetics of iron uptake in *Magnetospirillum gryphiswaldense*. Arch. Microbiol. 166, 301–307.

Schüler, D., Baeuerlein, E., 1998. Dynamics of iron uptake and Fe_3O_4 biomineralization during aerobic and microaerobic growth of *Magnetospirillum gryphiswaldense*. J. Bacteriol. 180, 159–162.

Stoltz, J.F., Chang, S.B.R., Kirschvink, J.L., 1986. Magnetotactic bacteria and single-domain magnetite in hemipelagic sediments. Nature 321, 849–851.

Tarduno, J.A., 1992. Magnetic susceptibility cyclicity and magnetic dissolution in Cretaceous limestones of the Southern Alps (Italy). Geophys. Res. Lett. 19, 1515–1518.

Tarduno, J.A., 1994. Temporal trends of magnetic dissolution in the pelagic realm: gauging paleoproductivity? Earth Planet. Sci. Lett. 123, 39–48.

Tarduno, J.A., Wilkison, S., 1996. Non-steady state magnetic mineral reduction, chemical lock-in, and delayed remanence acquisition in pelagic sediments. Earth Planet. Sci. Lett. 144, 315–326.

Tarduno, J.A., Tian, W., Wilkison, S., 1998. Biogeochemical remanent magnetization in pelagic sediments of the western equatorial Pacific Ocean. Geophys. Res. Lett. 25, 3987–3990.

Tauxe, L., Hartl, P., 1997. 11 million years of Oligocene geomagnetic field behaviour. Geophys. J. Int. 128, 217–229.

Vali, H., Förster, O., Amarantidis, G., Petersen, N., 1987. Magnetotactic bacteria and their magnetofossils in sediments. Earth Planet. Sci. Lett. 86, 389–400.

Villa, G., Fioroni, C., Pea, L., Bohaty, S., Persico, D., 2008. Middle Eocene-Late Oligocene climate variability: calcareous nannofossil response at Kerguelen Plateau, Site 748. Mar. Micropal. 69, 173–192.

Weiss, B.P., Kim, S.S., Kirschvink, J.L., Kopp, R.E., Sankaran, M., Kobayashi, A., Komeili, A., 2004. Ferromagnetic resonance and low temperature magnetic tests for biogenic magnetite. Earth Planet. Sci. Lett. 224, 73–89.

Yamazaki, T., 2009. Environmental magnetism of Pleistocene sediments in the North Pacific and Ontong-Java Plateau: temporal variations of detrital and biogenic components. Geochem. Geophys. Geosyst. 10, Q07Z04. doi:10.1029/2009GC002413.

Yamazaki, T., Kawahata, H., 1998. Organic carbon flux controls the morphology of magnetofossils in sediments. Geology 26, 1064–1066.

Yamazaki, T., Sølheid, P., 2011. Maghemite-to-magnetite reduction across the Fe-redox boundary in a sediment core from the Ontong-Java Plateau: influence on relative palaeointensity estimation and environmental magnetic application. Geophys. J. Int. 185, 1243–1254.